Reviews on Advanced Materials and Technologies, 2025, vol. 7, no. 4, pp. 211–221
DOI: 10.17586/2687-0568-2025-7-4-211-221

Critical Analysis of Clathrate Hydrate Formation, Growth and Dissociation Models

N.A. Shostak*

Kuban State University, 149 Stavropol'skaya str., Krasnodar, 350040, Russia

Article history

Received November 05, 2025
Received in revised form,
November 26, 2025
Accepted November 28, 2025
Available online December 03, 2025

Abstract

The study presents a comprehensive analysis of the existing physical and mathematical models describing the formation, growth, and dissociation of clathrate hydrates—complex condensed systems exhibiting hierarchical phase transitions across multiple spatial and temporal scales. The review systematizes thermodynamic, kinetic, molecular-dynamic, and hybrid approaches, emphasizing their theoretical foundations, applicability, and limitations. It is shown that despite decades of progress, existing models remain fragmented across scales and mechanisms. The absence of a unified description capable of linking molecular parameters, interparticle potentials, and macroscopic kinetic and thermobaric properties limits the predictability of hydrate behavior under both natural and technological conditions. The analysis is based on the comparative assessment of governing equations, physical assumptions, and scalability criteria of different model classes. The work substantiates the necessity of developing an integrative physical–mathematical framework combining equilibrium thermodynamics, transport phenomena, and non-equilibrium kinetics to adequately describe hydrate systems across formation and dissociation cycles.

Keywords: Clathrate hydrates; Thermodynamic modeling; Kinetic modeling; Molecular dynamics; Self-preservation

1. INTRODUCTION

Clathrate hydrates are crystalline inclusion compounds in which gas molecules are trapped within hydrogen-bonded cages of water molecules [1–3]. Beyond applications in gas transport and storage, they have become an important object of condensed matter physics, owing to the interplay between molecular interactions, structural ordering, and metastable behavior [4,5].

Hydrate systems exhibit hierarchical organization: processes occur across scales from picometers and femtoseconds (atomic vibrations, proton transfer) to millimeters and hours (macroscopic hydrate plug formation in pipelines); see Fig. 1. Thermodynamics determines the direction and feasibility of transformations, while kinetics and microstructure define actual pathways and rates [3,6].

However, existing theoretical approaches tend to address these levels separately, hindering a unified understanding of hydrate phase behavior under variable thermobaric conditions [7,8]. Despite extensive experimental and modeling efforts, current frameworks still inadequately connect molecular-level phenomena with macroscopic kinetic observables [9–11].

This review provides a systematic analysis of classical and modern models of hydrate formation, growth, and dissociation, emphasizing their physical foundations, assumptions, and intrinsic limitations [12–14].

2. MODELS OF HYDRATE FORMATION

2.1. Historical and conceptual development

A chronological analysis shows a stepwise evolution of the understanding of hydrate formation processes (Fig. 2):

1) Empirical–thermodynamic stage (up to the 1950s): by the accumulation of equilibrium data and phenomenological treatment within classical thermodynamics. Early models (e.g., Roozeboom-type diagrams) delineated hy-

* Corresponding author: N.A. Shostak, e-mail: nikeith@mail.ru

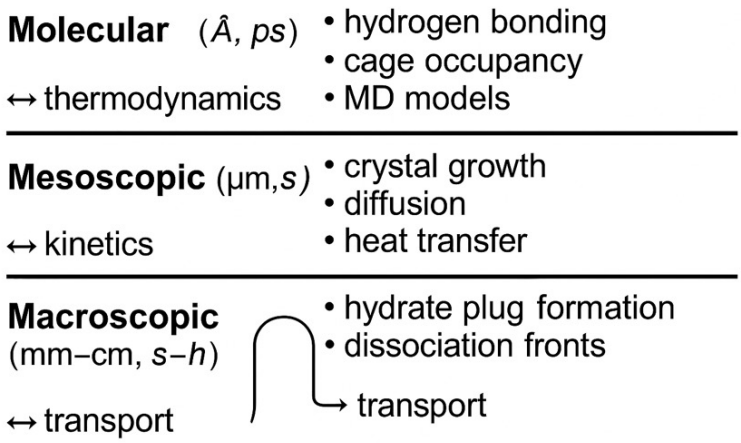

Fig. 1. Hierarchical structure and processes in clathrate hydrate systems.

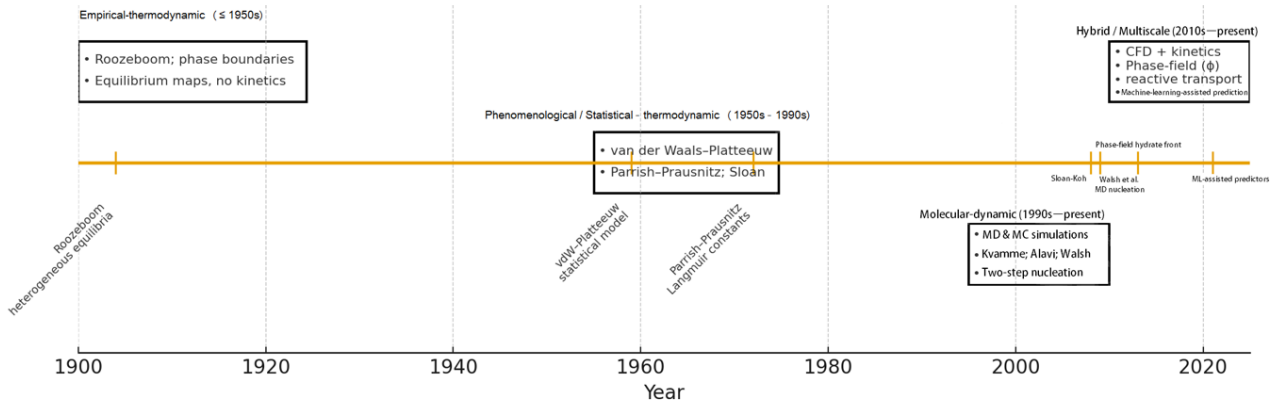

Fig. 2. Chronological evolution of theoretical and computational models of hydrate formation and dissociation.

drate stability boundaries without clarifying formation mechanisms [12].

2) Phenomenological stage (1950s–1990s): by the advent of statistical-thermodynamic models, most notably the van der Waals-Platteeuw theory [1] and its modifications by Parrish and Prausnitz [2], Sloan [3], and others. These models, based on probabilistic cage occupancy, enabled quantitative equilibrium predictions but ignored kinetics and nucleation. Key refinements included empirical Langmuir-constant correlations [2], improved expressions for the chemical potential of water in asymmetric mixtures [13], and accounting for guest non-sphericity and multi-shell interactions [14]. Chen and Guo [6] extended the model to systems with inhibitors such as methanol, while Du and Guo [15] critically revised the Langmuir analogy. Kvamme and Tanaka [16] expanded the theory to other guest molecules (C_2H_4, C_2H_6, CO_2).

3) Molecular-dynamics stage (from the 1990s to the present): associated with advances in computational physics and the realization that hydrate formation is a complex non-equilibrium self-organization process. The advent of powerful computational methods (molecular dynamics, Monte Carlo) made it possible to move from describing states to simulating the dynamics of the process at the molecular [10,11,17–19].

Parallel kinetic models (Englezos-Bishnoi [4], Kashchiev [20]) described macroscopic growth rates via mass-transfer equations.

Since the first statistical-thermodynamic phase-equilibrium model of hydrates [1], more accurate predictive models have been proposed. Parrish and Prausnitz [2] used an empirical correlation to compute the Langmuir constant, which greatly simplified the application of the van der Waals-Platteeuw framework. A key drawback of the van der Waals-Platteeuw model is its weak ability to predict hydrate formation at extreme (high and low) pressures and temperatures [3]. To overcome the inadequacy of the Parrish-Prausnitz approach for asymmetric mixtures, Ng and Robinson [13] modified the chemical potential of water in the hydrate phase, improving predictive performance. John et al. [14] noted the effect of non-spherical and external water molecules in guest species on the overall cavity potential energy. They used a three-layer spherical model to describe interactions between guest molecules in a hydrate cavity and the surrounding water molecules and introduced a correction factor to account

for non-sphericity. Chen and Guo [6] refined the model of John et al. and predicted hydrate formation conditions in a system containing methanol. Du and Guo [15] argued that the analogy between the encapsulation of gas molecules by water and Langmuir isothermal adsorption is not as close as van der Waals and Platteeuw assumed and therefore proposed a new model. Kvamme and Tanaka [16] extended the van der Waals-Platteeuw theory to study the thermodynamic stability of C_2H_4, C_2H_6, CO_2.

Methods for predicting hydrate phase equilibria mainly include the enthalpy-entropy diagram method, thermodynamic modeling, and neural-network algorithms. The enthalpy-entropy diagram method [9] is the earliest of these but lacks structural insight into hydrates, leading to significant errors. Neural-network approaches employing multilayer perceptrons and radial basis functions have become increasingly popular in recent years, yet they remain applicable only to specific hydrate formers [17].

Each stage broadened the interpretive base; nevertheless, none has produced a reproducible, scalable description of the full "formation-growth-dissociation" cycle over wide thermobaric ranges and multicomponent mixtures [18]. This is due to fragmented treatment of non-equilibrium kinetics and heat/mass-transfer conditions, strong dependence on empirical coefficients and calibration, and persistent scaling problems [21].

Consequently, there is a need for a systemic, integrative (hybrid) physical-mathematical apparatus that links molecular parameters and intermolecular potentials with macroscopic thermobaric and kinetic characteristics of hydrate processes [22].

Thus, the evolution of hydrate modeling reflects the broader transition in condensed matter physics-from equilibrium-based description toward multiscale and non-equilibrium frameworks.

2.2. Classification of existing models

According to the generalized analysis, models of hydrate formation processes can be conditionally divided into four main classes (Table 1). The approaches to describing hydrate formation and growth can be grouped as follows:

– thermodynamic models based on equations of state and phase-equilibrium descriptions;

– kinetic models that simulate nucleation and crystal growth rates based on energetic barriers;

– molecular-dynamic models relying on direct simulation of intermolecular interactions and structure formation;

– hybrid models combining macroscopic and microscopic descriptions.

While such classification delineates the methodological diversity, it also exposes the fundamental fragmentation of hydrate theory: no existing framework consistently bridges microscopic interactions with macroscopic thermodynamic observables.

Thermodynamic models correctly describe equilibrium but ignore nucleation; kinetic models require empirical coefficients and are sensitive to experimental conditions; molecular-dynamic models are limited by small scales and high computational cost; hybrid models have yet to achieve universal predictive capability. These limitations arise because each model addresses only a single hierarchical level-molecular, mesoscopic, or macroscopic. A correct description of the entire hydrate-formation cycle requires unifying these levels within a single physical-mathematical framework, which is the aim of the present work.

2.3. van der Waals-Platteeuw model

The van der Waals-Platteeuw model [1] introduced a consistent statistical-mechanical description of hydrates as solid solutions of inclusion, forming the foundation of modern hydrate thermodynamics.

It assumes that:

– the hydrate lattice is a crystalline water framework with two sublattices (small and large cages);

– each cavity hosts at most one guest molecule;

– guest-guest interactions are negligible.

Table 1. Classification of existing hydrate-formation models.

Model type	Principle and key representatives	Advantages	Limitations and drawbacks
Thermodynamic	van der Waals-Platteeuw [1], Parrish & Prausnitz [2], Sloan [3]	Accurate equilibrium prediction	Ignores kinetics and metastability
Kinetic	Englezos & Bishnoi [4], Kashchiev [20], Byk [23]	Describes growth rates	Empirical coefficients, system-specific
Molecular dynamic	Alavi & Ripmeester [11], Walsh et al. [10]	Atomistic mechanism	Limited by scale and computation
Hybrid / multiscale	Kvamme [8], Sloan-Koh [3], Uchida et al. [24]	Accounts for mass/heat transport and morphology	Requires parameter fitting; lacks universality

The model is based on calculating the chemical potential of water μ_H in the hydrate phase relative to its chemical potential μ_β in an empty (hypothetically stable) lattice:

$$\mu_H(T,P) = \mu_\beta(T,P) + R \cdot T \sum_i \nu_i \cdot \ln\left(1 - \sum_i \theta_{ij}\right). \quad (1)$$

Here ν_i is the number of cavities of type i (small, large) per water molecule in the lattice; R is the universal gas constant; T is temperature; and θ_{ij} is the occupancy of a cavity of type i by a guest of type j:

$$\theta_{ij} = \frac{C_{ij}(T) \cdot f_i}{1 + \sum_k C_{ij}(T) \cdot f_k}, \quad (2)$$

where f_j is the fugacity of component j in the gas phase (computed from an equation of state), and $C_{ij}(T)$ is the Langmuir constant characterizing the strength of guest-cavity interactions as a function of temperature, determined from the guest–cavity potential $\omega_{t,i}(r)$ as

$$C_{ij}(T) = \frac{4\pi}{k_B T} \int_0^R r^2 \exp\left[-\frac{\omega_{t,i}(r)}{k_B T}\right] dr, \quad (3)$$

Equilibrium between the hydrate (H) and aqueous (L_w) phases is described by the iteratively solved equality of the chemical potentials of water:

$$\mu_H(T,P,\theta_{ij}) = \mu_L(T,P). \quad (4)$$

The inputs are thermobaric conditions, gas composition, salinity, potentials, and the equation of state.

Among the limitations are the neglect of kinetics and metastability and sensitivity to the choice of the guest–cavity potential and the equation of state.

2.4. Kinetic models of hydrate formation

Based on Fick's law and the assumption of dominant mass-transfer effects driven by the difference in fugacity between the hydrate-forming system and equilibrium conditions, the hydrate growth rate (per particle, in terms of overall driving force) is given by [4]:

$$\left(\frac{dn}{dt}\right)_P = K \cdot A(f - f_0), \quad (5)$$

$$r(t) = \int_0^\infty \left(\frac{dn}{dt}\right)_P \varphi(r,t)\, dr = 4\pi K \mu_2 (f - f_0), \quad (6)$$

$$\mu_2 = \int_0^\infty r^2 \varphi(r,t)\, dr, \quad (7)$$

$$r \approx \frac{D}{y}(C - C_s), \quad (8)$$

where n is the moles of gas incorporated into hydrate over time t; A is the surface area (m^2) of a nucleation core; K is a parameter (mol/(m^2·MPa·s)) characterizing interfacial mass transfer at the core surface; f and f_0 are the gas fugacities (MPa) in the hydrate-forming system and at equilibrium, respectively; r is a characteristic core size (m); $\varphi(r,t)$ is the size distribution function (m^{-4}); μ_2 is the distribution of nucleation-core sizes (m^2/m^3); D is the diffusion coefficient of gas in water; y is the thickness of the diffusion boundary layer at the core surface; C is the concentration of guest molecules in the bulk water; and C_s is the gas concentration in the immediate vicinity of the nucleation core.

Byk et al. [23] proposed a relation for the time τ required for complete conversion of the gas in a bubble into hydrate:

$$\tau = \frac{6\Delta H P d}{z T_1 K (T_1 - T_2) R}, \quad (9)$$

where ΔH is the heat (J/mol) of hydrate formation; P is the equilibrium hydrate-formation pressure (Pa); R is the universal gas constant (J/(mol·K)); z is the gas compressibility factor; d is the bubble diameter (m); K is the heat-transfer coefficient (J/(m^2·s·K)); T_1 is the hydrate-formation temperature (K); and T_2 is the equilibrium temperature (K) of the water surrounding the bubble.

According to Eq. (9), τ is directly proportional to bubble diameter. However, this contradicts gas mass transfer into a liquid across a spherical interface, which depends quadratically on diameter. The contradiction stems from an incorrect identification of the rate-limiting step.

The effect of thermal conductivity is accounted for by the relation [23]:

$$\tau_t = \frac{P r_0^2 \Delta H}{6k \Delta t z R T}\left(1 - \frac{3r_h^2}{r_0^2} + \frac{2r_h^3}{r_0^3}\right), \quad (10)$$

where ΔH is the heat of hydrate formation; k is the thermal conductivity of hydrate (for methane hydrate ≈ 0.2 J/(m·s·K)); and Δt is the mean temperature difference (K).

The relative roles of diffusion and thermal conductivity in hydrate-formation time are evaluated by:

$$\frac{\tau}{\tau_t} = \frac{nk\Delta t}{D\Delta f \Delta H}. \quad (11)$$

It is noted that diffusion plays the determining role in hydrate formation.

Hydrate-film growth M_H (kg/s) at a water surface is determined by [23]:

$$M_H = \pi \cdot h \cdot \rho \cdot \upsilon_r^2 \cdot J \cdot \tau, \quad (12)$$

$$\upsilon_r = a \cdot \exp\left(\frac{\Delta T \cdot b}{10P}\right), \quad (13)$$

$$J = c \cdot \exp\left(-\frac{\Delta T \cdot u}{20\sqrt{P}}\right)\sqrt{T}, \quad (14)$$

where h is the thickness (mm) of the forming hydrate film; ρ is hydrate density; υ_r is the radial growth rate (mm/s)

of the hydrate film at the gas-water interface; J is the nucleation rate of methane hydrate [1/(cm^2·min)] at the free gas-water interface as a function of pressure P (MPa) and undercooling ΔT; *a, b, c, u* are empirical coefficients depending on system pressure; and τ is the contact time (s).

The rate of hydrate accumulation during volumetric formation at a hydrate surface can be written as the mass flux of water M_ω through a planar hydrate film of thickness h and area F

$$M_\omega = D_\omega \frac{F\Delta f \rho_\omega}{h}. \quad (15)$$

Here D_ω is the diffusion coefficient of water through the hydrate film (for methane hydrate $D_\omega \sim 5\times10^{-6}$–$10^{-8}$ cm^2/s; for natural gas with relative density of 0.6 $D_\omega \approx 10^{-6}$ cm^2/s); Δf is the difference in water-vapor fugacity over liquid water and over hydrate; ρ_ω is the density of water in the hydrate state (0.792–0.757); and h is the hydrate-film thickness after time τ:

$$h = \sqrt{\frac{2D\Delta f \tau}{n}}, \quad (16)$$

where n is the hydrate number.

Such inconsistencies highlight the need for more rigorous multiscale coupling between diffusion, heat transfer, and interfacial kinetics.

2.5. Mesoscopic diffusion-based models

Mesoscopic diffusion-based models provide a bridge between statistical–thermodynamic descriptions and macroscopic kinetic formulations, explicitly resolving diffusion-controlled transformation of ice or water into hydrate. Assuming that diffusion drives the transformation of ice into hydrate, Groysman derived [25]:

$$\tau = \frac{r_0^2}{6D}\frac{x_f}{1-x_f}, \quad (17)$$

$$x_f = x(\xi,\tau) = \frac{M_g}{M_g + nM_w}, \quad (18)$$

where τ is the time (s) to transform an ice sphere of radius r_0 (m) into hydrate; D is the diffusion coefficient of gas in hydrate (10^{-14} m²/s); x_f is the gas concentration in the sphere (fraction); ξ is the thickness of the ice layer converted to hydrate at the sphere surface; M_g and M_w are the molar masses of gas and water; and n is the current hydrate number.

In Ref. [26] it is assumed that during hydrate formation the outer surface grows by adsorbing gas molecules. The mass Δm_g of gas incorporated into hydrate during time $\Delta\tau$ is given by:

$$\Delta m_g = -D\frac{\Delta\rho}{\lambda}S\Delta\tau, \quad (19)$$

$$D = \lambda\omega = 2a\exp\left(\frac{\Delta H_u m}{zRT}\right)\beta_r \frac{V}{S}, \quad (20)$$

$$\lambda = 2a\exp\frac{\varepsilon_s}{2kT} = 2a\exp\frac{\Delta H m}{zRT\gamma}, \quad (21)$$

where S is the area (m^2) of the adsorption layer; $\Delta\rho$ is the difference between the gas density above and within the adsorption layer; λ is the molecular diffusion path (m); ω is a characteristic diffusion velocity (m/s); a is the hydrate lattice parameter (m); ΔH_u is the specific heat of gas sublimation (J/kg; for propane and butane, 426.5 and 386 kJ/kg, respectively); ΔH is the heat of hydrate formation (J/kg); m is molar mass (kg/mol); z is the gas compressibility factor; R = 8.31441 J/(mol·K) is the universal gas constant; T is temperature (K); ε_s is the adsorption energy (approximated by the experimentally determined sublimation heat per particle, accounting for the number of bonds); k is the Boltzmann constant; β_r is a crystallographic kinetic coefficient; V is gas volume in the reactor (m^3); and γ is the number of hydrate faces.

These findings established the concept of a two-step nucleation mechanism — amorphous clustering followed by structural ordering — now widely accepted in hydrate nucleation theory.

2.6. Molecular dynamic models

Molecular dynamic (MD) simulations provide a direct, atomistic-level description of hydrate nucleation and early-stage growth, complementing thermodynamic and continuum kinetic models. In contrast to phenomenological approaches, MD resolves the trajectories of individual water and guest molecules under a prescribed intermolecular potential and thus can explicitly capture local structuring, cage formation, and transient defects.

Early MD studies focused on the spontaneous nucleation of methane hydrates from supersaturated aqueous solutions or water–gas interfaces. Walsh et al. [10] performed microsecond-scale simulations that revealed a two-step nucleation mechanism: (i) formation of dense amorphous, hydrate-like clusters enriched in guest molecules, followed by (ii) gradual structural ordering into crystalline clathrate cages. This picture differs markedly from classical nucleation theory, which assumes the direct appearance of a crystalline nucleus with bulk-like symmetry.

Subsequent work has examined guest migration, cage-to-cage hopping, and local rearrangements in pre-formed hydrate frameworks. Alavi and Ripmeester [11], using atomistic simulations of hydrogen migration through clathrate cages, demonstrated the importance of transient cage distortions and local hydrogen-bond rearrangements for transport in the solid phase. Although that study was not exclusively devoted to hydrate nucleation, it is representative of a broader class of MD investigations that probe local dynamics

within the hydrate lattice, including diffusion of guest molecules, defect formation, and mechanical response.

From the modeling standpoint, MD studies have established several key features now widely accepted in hydrate nucleation theory [10,11,26]:

– hydrate nucleation is non-classical and proceeds via disordered, amorphous precursors rather than direct formation of an ideal crystalline nucleus;

– water molecules in the pre-nucleation clusters exhibit partial hydrate-like ordering of hydrogen bonds, while the network remains dynamically fluctuating;

– guest molecules play a dual role, both stabilizing emerging cages via dispersion interactions and enhancing local density fluctuations;

– the effective nucleation barrier is sensitive to supersaturation, cooling rate, system size, and the presence of interfaces or impurities.

Despite these advances, MD simulations remain limited by accessible time and length scales. Even with specialized algorithms and enhanced-sampling techniques, simulations are typically restricted to nanometer–micrometer and nanosecond–microsecond regimes, which is several orders of magnitude shorter than macroscopic hydrate formation in pipelines and porous media. Therefore, MD results are mostly used to:

– validate and refine coarse-grained kinetic models (e.g., the two-step nucleation concept introduced into continuum descriptions);

– parameterize phenomenological rate expressions (e.g., activation energies and pre-exponential factors in hybrid models [8,27]);

– provide microscopic justification for assumptions about local structure, cage occupancy, and defect-mediated mechanisms.

2.7. Hybrid and multiscale models

In the hybrid model [8,27], the classical van der Waals-Platteeuw thermodynamic model is used to calculate the driving force $\Delta\mu$, while surface kinetics are introduced via an activation barrier (Arrhenius-type):

$$\frac{dn}{dt} = k_0 \cdot A \exp\left(-\frac{E_a \Delta\mu}{RT}\right)\left(\frac{\Delta\mu}{RT}\right)^m, \quad (22)$$

where k_0 is the pre-exponential (Arrhenius) factor (m/(s·Pa)); E_a is the activation energy (J/mol) of the elementary formation act; and m is an empirical exponent (1–2). The activation energy is parameterized using molecular dynamics data. The model is semi-empirical, and the accessible time scale is limited to minutes.

In the Sloan-Koh framework [3], thermodynamic calculations using the van der Waals-Platteeuw model to determine equilibrium temperature are combined with the Englezos-Bishnoi kinetic equation for growth rate [4]:

$$\frac{dn}{dt} = k_0 \cdot A \exp\left(-\frac{E_a}{RT}\right)\left[1 - \frac{P}{P_{eq}(T)}\right]^m, \quad (23)$$

Multilevel phase-field models [16,24] describe the propagation of the hydrate front via an order parameter φ coupled to heat and mass transport equations:

$$\frac{d\varphi}{dt} = -M\frac{\partial F}{\partial \varphi}, \quad (24)$$

$$F = \int\left[f(\varphi) - \Delta\mu\varphi + \frac{\kappa}{2}\left|\nabla\varphi\right|^2\right]dV, \quad (25)$$

where M is the phase mobility related to kinetics ($m^3/(J\cdot s)$); κ is the interfacial-energy coefficient (J/mol); and $f(\varphi)$ is a potential defining the stable states.

In recent years, hybrid models have been further extended using computational fluid dynamics and reactive transport modeling, enabling the simulation of hydrate processes in porous and geological media.

2.8. Key physical problems identified from model analysis

1. **Nucleation mechanism**. Existing kinetic models postulate "nucleation cores" with a prescribed size distribution but do not describe their molecular origin. MD studies [10,11,26] show a local-ordering two-step mechanism: dense amorphous clusters form first and then crystallize-absent in classical models.

2. **Rate-limiting step ambiguity**. Models of growth from a gas bubble and on a solid surface rely on different assumptions (diffusion, heat transfer, surface kinetics), leading to divergent predictions [4,22,23].

3. **Metastability and self-organization.** None of the considered models adequately reproduces experimentally observed metastable states and self-preservation effects due to the neglect of nonlinear system dynamics and the evolution of an order parameter quantifying hydrate-phase ordering [5,7,28]. From the standpoint of condensed matter physics, such metastable ordering may be interpreted as a non-equilibrium steady state stabilized by the formation of low-diffusivity boundary phases.

Prospects: the need for a systemic-integrative approach. The analysis demonstrates that each model class treats only one hierarchical level-molecular, mesoscopic, or macroscopic. A correct description of the entire hydrate-formation cycle requires unifying these levels within a single physical–mathematical apparatus.

3. MODELS OF HYDRATE DISSOCIATION

Hydrate dissociation (decomposition) is not a simple reverse phase transition but a complex multistage process proceeding under strongly non-equilibrium conditions. Its adequate mathematical description is critical for applied problems such

as gas field development and transportation, water desalination, and gas-mixture separation [19,26,28]. However, current models largely focus on equilibrium boundaries, while the physical aspects of kinetics and, especially, metastable hydrate states remain insufficiently studied and formalized.

3.1. Physical nature and staging of dissociation

Unlike equilibrium formation, dissociation is initiated by removing the system from equilibrium and proceeds through the following stages:

1) Heat input and/or pressure reduction-driving force determining the thermodynamic potential of decomposition;

2) Destabilization of the crystal lattice-at the molecular level, breaking of van der Waals interactions holding guest molecules in cages and reorganization of hydrogen bonds in the water framework;

3) Growth of the dissociation front-starts at the crystal surface or defects and propagates inward as a moving "hydrate-product" interface;

4) Diffusion of released gas through the layer of decomposition products (water, ice, or a new hydrate film) into the free volume;

5) Removal of decomposition products-at the macroscopic level, this sets the overall rate, which may be limited by intrinsic decomposition kinetics (stages 2–3) or by heat and mass transfer (stages 1,4–5).

Depending on dominant resistance, dissociation may be controlled by intrinsic kinetics or heat/mass transfer [23,29–31].

Existing models are generally phenomenological, expressing the dissociation rate as a function of pressure or temperature difference, without exposing the molecular or mesoscopic mechanisms. Despite their diversity, most dissociation models remain phenomenological and system-specific, highlighting the need for a generalized non-equilibrium theory.

3.2. Self-preservation and metastable states

A key manifestation of the complex nature of dissociation is the self-preservation effect, first described in detail by Davidson et al. [32] and Yakushev and Istomin [19]. The phenomenon consists in an anomalously low dissociation rate within a temperature region where, according to equilibrium thermodynamics, hydrate should be unstable.

The mechanism is attributed to the formation of a dense, low-permeability barrier film on the dissociating hydrate surface. Depending on conditions, this film may be:

1) an ice layer formed by freezing of released water;

2) a dense hydrate film with altered properties;

3) a hybrid of hydrate and ice phases.

This film kinetically "locks" the bulk hydrate, creating a significant barrier to gas diffusion and/or heat flow, thereby stabilizing a metastable hydrate state over long periods. This effect explains natural relict hydrates outside classical stability zones. From the standpoint of condensed matter physics, self-preservation exemplifies a metastable phase stabilized by kinetic constraints, where relaxation to the global free-energy minimum (gas + ice) is greatly slowed by an intermediate barrier structure.

3.3. Analysis of existing dissociation models

3.3.1. Surface-kinetic model

The Englezos–Bishnoi [4] model assumes that dissociation is limited by the elementary lattice-breakdown step at the phase boundary. For methane hydrate, the rate equation is:

$$\frac{dn}{dt} = k \cdot A\left(P_{eq} - P\right)^m, \tag{26}$$

where n is the moles of released gas; k is the kinetic constant (m/(s·Pa)); A is the active surface area (m^2); P_{eq} is the equilibrium pressure at the given temperature; P is the current gas pressure; and m is an empirical exponent (typically 1–2).

Temperature dependence follows Arrhenius:

$$k = k_0 \exp\left(-\frac{E_a}{RT}\right), \tag{27}$$

where $E_a \approx 30$–50 kJ/mol; R is the gas constant; T is temperature (K).

The model applies to thin samples with good heat exchange and no barrier layer (e.g., rapid depressurization). It neglects coupled heat/mass transfer and is valid mainly at early dissociation. Phenomenological parameters (effective thermal conductivity, diffusion coefficient, kinetic constant) are condition-dependent and require experiment-specific calibration; the model cannot a priori predict self-preservation onset or duration.

3.3.2. Heat-limited (Stefan-type) models

This class includes the one-phase Stefan model [3,23], a two-phase variant accounting for heat transfer through water [29], dissociation under isobaric conditions with internal heating [24], and models including water phase transitions [30], as well as numerical/generalized Stefan-type models [8,31].

At low temperatures and for large hydrate volumes, the principal limitation is removal of the phase-transition heat. The moving-boundary problem reads:

$$\rho_h \cdot L \frac{dX}{dt} = -\lambda \left.\frac{\partial T}{\partial x}\right|_{x=X(t)}, \tag{28}$$

$$\frac{\partial T}{\partial x} = \alpha \frac{\partial^2 T}{\partial x^2}, \tag{29}$$

$$0 < x < X(t), \tag{30}$$

$$T(0,t) = T_\infty, \tag{31}$$

$$T\{X(t),T\} = T_m, \tag{32}$$

where $X(t)$ is the front position (m) at time t; ρ_h is hydrate density (kg/m^3); L is the specific heat of dissociation (~ 5.0×10^5 J/kg); λ is the effective thermal conductivity (W/(m·K)) of the product layer (water/ice); T_∞ is the boundary temperature (K); T_m is the interface temperature (K). The solution yields $X(t) \sim \sqrt{t}$, consistent with steady heating.

With an ice crust, additional thermal resistance is introduced:

$$R = \frac{\delta_{ice}}{\lambda_{ice}} + \frac{\delta_w}{\lambda_w}, \tag{33}$$

$$\frac{dX}{dt} = \frac{T_\infty - T_i}{\rho_h \cdot L \cdot R}, \tag{34}$$

where δ_{ice} and δ_w are the layer thicknesses (ice and water), and T_i is the temperature (K) at the inner boundary of the ice layer if a distinct ice phase exists between hydrate and water. These models apply to macroscopic samples, low temperatures, and weak gas diffusion; they do not describe mass transfer or structural evolution of the product layer.

3.3.3. Diffusion-limited models

When hydrate particles dissociate in media with poor heat transfer (water, gas), the rate is controlled by gas diffusion through the product layer. This class covers single-film diffusion through ice [19,28], spherical "shrinking core" models [22,29], and ice-permeation models [7,33].

Using the shrinking-core approximation:

$$\frac{dR}{dt} = -\frac{D}{\rho_h \cdot R}\left(C_s - C_\infty\right), \tag{35}$$

where R is the current hydrate-core radius (m); D is the effective diffusion coefficient (m²/s); and C_s, C_∞ are gas concentrations at the surface and in the bulk. Integration gives $(1-(R/R_0)^3) \propto t$.

These models describe regimes where transport through ice/water/porous media sets the rate. They are applicable to granular hydrates, porous matrices, and moderate pressures; however, achieving universality requires phase-field or multilevel formulations combining diffusion, heat transfer, and microstructural dynamics.

3.3.4. Barrier-layer model

Representative models include [7,26,32,34]. At $T < 273$ K and limited heating, an ice or dense hydrate film forms on the surface, impeding diffusion and heat removal. The dissociation rate is then:

$$m = \frac{D_f}{\delta} \cdot A(C_s - C_\infty), \tag{36}$$

$$\rho_h L \frac{dX}{dt} = -\frac{T_s - T_\infty}{R_t}, \tag{37}$$

where D_f is the effective gas diffusivity in the film (2–3 orders lower than in water); δ is film thickness (10^{-5}–10^{-4} m); R_t is the thermal resistance of the film; and T_s, T_∞ are the surface and ambient temperatures (K).

Film thickness evolves as:

$$\frac{d\delta}{dt} = K_f\left(1 - \frac{T}{T_m}\right) - K_m(T - T_m), \tag{38}$$

where K_f and K_m are formation and melting constants; T_m is the melting temperature (K).

These models apply to low-temperature dissociation with extended stability plateaus.

3.3.5. Front-propagation (phase-field) models

A phase-field approach captures the moving "hydrate–product" boundary and non-equilibrium morphology. Introducing the order parameter $\varphi(r,t)$:

$$\frac{d\varphi}{dt} = -M\frac{\partial F}{\partial \varphi}, \tag{39}$$

$$F = \int\left[\frac{\kappa}{2}|\nabla\varphi|^2 + f\left(\varphi;T,P,\Delta\mu\right)\right]dV, \tag{40}$$

where M is mobility linked to decomposition kinetics; κ is interfacial energy; $f(\varphi)$ sets stable states (hydrate vs products); $\Delta\mu$ is a chemical-potential difference.

Coupled heat and mass transport:

$$\rho \cdot c_P \frac{\partial T}{\partial t} = \nabla\left(\lambda\nabla T\right) - L\frac{\partial\varphi}{\partial t}, \tag{41}$$

$$\frac{\partial c}{\partial t} = \nabla\left(D\left(\varphi\right)\nabla c\right). \tag{42}$$

These models capture morphology, front dynamics, and transitions between equilibrium behavior and self-preservation.

3.3.6. Molecular dynamics simulations

Molecular dynamics simulations of hydrate dissociation focus primarily on the microscopic evolution of the hydrate–water–ice interface and the behavior of guest molecules during decomposition. Although such simulations are constrained by time and length scales, they provide unique information on mechanisms that cannot be accessed directly in experiments.

Atomistic studies show that, upon heating or depressurization, dissociation begins with local destabilization of cages at the surface, followed by cooperative breaking of hydrogen bonds and escape of guest molecules into

Table 2. Comparison of applicability and limiting factors.

Model type	Limiting factor	Scale	Typical T range
Surface-kinetic	Lattice breakdown	Micro-meso	270–285 K
Heat-limited (Stefan)	Heat supply	Meso	250–273 K
Diffusion-limited	Gas transport	Meso	260–280 K
With barrier film (self-preservation)	Diffusion & heat through barrier	Macro	240–273 K
Phase-field	Front dynamics, morphology	Meso-macro	250–290 K

surrounding water or gas. In agreement with experimental observations of self-preservation [7,28,34,35], MD indicates that released water can rapidly reorganize into an ice-like shell with reduced permeability, partly blocking further gas diffusion and heat transfer.

Simulations of guest migration in intact hydrates [11] also help to interpret the early stages of dissociation: local cage distortions, defect formation, and transient channels for molecular transport become increasingly frequent as the system is driven away from equilibrium. These microscopic events underpin the effective parameters used in continuum models (diffusion coefficients in ice and hydrate, interfacial kinetic constants, etc.), but are not explicitly resolved in Stefan-type or diffusion-limited descriptions.

Due to computational cost, MD cannot yet reproduce the full evolution of a macroscopic sample over experimental time scales. Its role in dissociation modeling is therefore supporting and interpretative: MD provides:

– microscopic mechanisms for surface cage breakdown and guest release;

– qualitative and semi-quantitative estimates of local transport coefficients;

– insight into how structural heterogeneities and defects contribute to metastability and self-preservation under sub-equilibrium conditions.

These results justify the use of effective barrier layers, reduced diffusivities, and history-dependent kinetic coefficients in macroscopic dissociation models considered in Sections 3.3.2–3.3.5.

3.4. Comparison of applicability and limiting factors

Existing dissociation models span molecular to macroscopic scales and differ by rate-limiting mechanisms (Table 2).

4. CONCLUSION

The evolution of hydrate modeling — from empirical correlations to hybrid multiscale frameworks — illustrates the ongoing convergence of thermodynamics, kinetics, and condensed matter physics. However, current approaches fail to describe the entire life cycle of hydrate systems, especially in metastable regimes. Bridging molecular-scale processes with macroscopic observables through physically consistent mathematical formulations remains the core challenge and research frontier.

REFERENCES

[1] J.H. van der Waals, J.C. Platteeuw, Clathrate solutions, *Advances in Chemical Physics*, 1959, vol. 2, pp. 2–57.

[2] W.R. Parrish, J.M. Prausnitz, Dissociation pressures of gas hydrates formed by gas mixtures, *Industrial & Engineering Chemistry Process Design and Development*, 1972, vol. 11, pp. 26–35.

[3] E.D. Sloan, C.A. Koh, *Clathrate Hydrates of Natural Gases (3rd ed.)*, CRC Press, Boca Raton, 2008, 752 p.

[4] P. Englezos, N. Kalogerakis, P.D. Dholabhai, P.R. Bishnoi, Kinetics of formation of methane and ethane gas hydrates, *Chemical Engineering Science*, 1987, vol. 42, no. 11, pp. 2647–2658.

[5] M. Mohamadi-Baghmolaei, A. Hajizadeh, R. Azin, A.A. Izadpanah, Assessing thermodynamic models and introducing novel method for prediction of methane hydrate formation, *Journal of Petroleum Exploration and Production Technology*, 2018, vol. 8, pp. 1401–1412.

[6] G.J. Chen, T.M. Guo, Thermodynamic modeling of hydrate formation based on new concepts, *Fluid Phase Equilibria*, 1996, vol. 122, no. 1–2, pp. 43–65.

[7] A. Falenty, W.F. Kuhs, "Self-preservation" of CO_2 gas hydrates: surface microstructure and ice perfection, *The Journal of Physical Chemistry B*, 2009, vol. 113, no. 49, pp. 15975–15988.

[8] B. Kvamme, Kinetics of hydrate formation, dissociation and reformation, *Results in Engineering*, 2021, vol. 1–2, art. no. 100004.

[9] D.L. Katz, *Handbook of Natural Gas Engineering*, McGraw-Hill, New York, 1959.

[10] M.R. Walsh, C.A. Koh, E.D. Sloan, A.K. Sum, D.T. Wu, Microsecond simulations of spontaneous methane hydrate nucleation, *Science*, 2009, vol. 326, no. 5956, pp. 1095–1098.

[11] S. Alavi, J.A. Ripmeester, Hydrogen-gas migration through clathrate hydrate cages, *Angewandte Chemie*, 2007, vol. 119, no. 32, pp. 6214–6217.

[12] H.W. Roozeboom, *Die heterogenen Gleichgewichte vom Standpunkte der Phasenlehre*, 3 vols., Wilhelm Engelmann, Leipzig, 1904–1910.

[13] H.-J. Ng, D.B. Robinson, Hydrate formation in systems containing methane, ethane, propane, carbon dioxide or hydrogen sulfide in the presence of methanol, *Fluid Phase Equilibria*, 1985, vol. 21, no. 1–2, pp. 145–155.

[14] V.T. John, K.D. Papadopoulos, G.D. Holder, A generalized model for predicting equilibrium conditions for gas hydrates, *AIChE Journal*, 1985, vol. 31, no. 2, pp. 252–259.

[15] Y. Du, T.M. Guo, Prediction of hydrate formation for systems containing methanol, *Chemical Engineering Science*, 1990, vol. 45, no. 4, pp. 893–900.

[16] B. Kvamme, H. Tanaka, Thermodynamic stability of hydrates for ethane, ethylene, and carbon dioxide, *The Journal of Physical Chemistry*, 1995, vol. 99, no. 18, pp. 7114–7119.
[17] Q. Nasir, H. Suleman, W.S. Abdul-Majeed, Application of machine learning on hydrate formation prediction of pure components with water and inhibitor solutions, *The Canadian Journal of Chemical Engineering*, 2024, vol. 102, no. 11, pp. 3953–3981.
[18] C.G. Xu, W. Zhang, H.Y. Li, C.W. Xiao, X.S. Li, A new way promoting hydrate formation with high energy efficiency and its effect mechanism, *SSRN Preprint*, 2022.
[19] V.A. Istomin, V.S. Yakushev, *Gas Hydrates in Natural Conditions* [Gazovye gidraty v prirodnykh usloviyakh], Nedra, Moscow, 1992 (in Russian).
[20] D. Kashchiev, A. Firoozabadi, Driving force for crystallization of gas hydrates, *Journal of Crystal Growth*, 2002, vol. 241, no. 1–2, pp. 220–230.
[21] B. Tohidi, A. Danesh, A. Todd, R. Burgass, Measurement and Prediction of Hydrate-Phase Equilibria for Reservoir Fluids, *SPE Production & Facilities*, 1996, vol. 11, no. 02, pp. 69–76.
[22] Y.F. Makogon, *Hydrates of Hydrocarbons*, PennWell Books, Tulsa, 1997.
[23] S.Sh. Byk, Y.F. Makogon, V.I. Fomina, *Gazovye Gidraty*, Nedra, Moscow, 1980, 296 p. (in Russian).
[24] T. Uchida, T. Ebinuma, J. Kawabata, H. Narita, Microscopic observations of formation processes of clathrate-hydrate films at an interface between water and carbon dioxide, *Journal of Crystal Growth*, 1999, vol. 204, no. 3, pp. 348–356.
[25] A.G. Groysman, Thermophysical Properties of Gas Hydrates [*Teplofizicheskie svoystva gazovykh gidratov*], Nauka, Novosibirsk, 1985, 95 p. (in Russian).
[26] A.B. Shabarov, A.V. Shirshova, M.Yu. Dan'ko, N.S. Komissarova, Experimental investigation of propane–butane gas hydrate formation, *Vestnik Tyumen State University*, 2009, no. 6, pp. 73–82 (in Russian).
[27] A. Svandal, B. Kvamme, Modeling the dissociation of carbon dioxide and methane hydrate using phase-field theory, *Journal of Mathematical Chemistry*, 2009, vol. 46, pp. 763–769.
[28] L.A. Stern, S. Circone, S.H. Kirby, W.B. Durham, Anomalous preservation of pure methane hydrate at 1 atm, *The Journal of Physical Chemistry B*, 2001, vol. 105, no. 9, pp. 1756–1762.
[29] H.C. Kim, P.R. Bishnoi, R.A. Heidemann, S.S.H. Rizvi, Kinetics of methane hydrate decomposition, *Chemical Engineering Science*, 1987, vol. 42, no. 7, pp. 1645–1653.
[30] M.H. Yousif, H.H. Abass, M. Selim, E.D. Sloan, Experimental and theoretical investigation of methane-gas-hydrate dissociation in porous media, *SPE Reservoir Engineering*, 1991, vol. 6, no. 1, pp. 69–76.
[31] T. Kawamura, M. Ohtake, Y. Sakamoto, Y. Yamamoto, H. Haneda, T. Komai, S. Higuchi, Experimental study of enhanced gas recovery from gas hydrate bearing sediments by inhibitor and steam injection methods, in: *Proceedings of the 6th International Conference on Gas Hydrates (ICGH 2008)*, Vancouver, Canada, 2008.
[32] D.W. Davidson, S.K. Garg, S.R. Gough, Y.P. Handa, C.I. Ratcliffe, J.A. Ripmeester, J.S. Tse, W.F. Lawson, Laboratory analysis of a naturally occuring gas hydrate from sediment of the Gulf of Mexico, *Geochimica et Cosmochimica Acta*, 1986. vol. 50, no. 4, pp. 619–623.
[33] V.A. Vlasov, Diffusion model of gas hydrate dissociation into ice and gas that takes into account the ice microstructure, *Chemical Engineering Science*, 2020, vol. 215, art. no. 115443.
[34] W.F. Kuhs, G. Genov, D.K. Staykova, T. Hansen, Ice perfection and onset of anomalous preservation of gas hydrates, *Physical Chemistry Chemical Physics*, 2004, vol. 6, no. 21, pp. 4917–4920.
[35] P. Englezos, Clathrate hydrates, *Industrial & Engineering Chemistry Research*, 1993, vol. 32, no. 7, pp. 1251–1274.

УДК 539.42:548.562

Критический анализ моделей образования, роста и диссоциации клатратных гидратов

Н.А. Шостак

ФГБОУ ВО «Кубанский государственный университет», Ставропольская ул., 149, Краснодар, 350040, Россия

Аннотация. В работе представлен комплексный анализ существующих физико-математических моделей, описывающих образование, рост и диссоциацию клатратных гидратов - сложных конденсированных систем, демонстрирующих иерархические фазовые переходы в различных пространственных и временных масштабах. В обзоре систематизированы термодинамические, кинетические, молекулярно-динамические и гибридные подходы, с акцентом на их теоретических основах, применимости и ограничениях. Показано, что, несмотря на десятилетия прогресса, существующие модели остаются фрагментированными по масштабам и механизмам. Отсутствие единого описания, связывающего молекулярные параметры, межчастичные потенциалы, макроскопические кинетические и термобарические свойства, ограничивает предсказуемость поведения гидратов как в природных, так и в технологических условиях. В работе обосновывается необходимость разработки интегративной физико-математической модели, объединяющей равновесную термодинамику, явления переноса и неравновесную кинетику для адекватного описания гидратных систем в циклах образования и диссоциации.

Ключевые слова: клатратные гидраты; термодинамическое моделирование; кинетическое моделирование; молекулярная динамика; самоконсервация